ACS APPLIED MATERIALS & INTERFACES

Research Article

www.acsami.org

Chiral Functionalization of Graphene Oxide by Optically Active Helical-Substituted Polyacetylene Chains and Its Application in Enantioselective Crystallization

Weifei Li, Junya Liang, Wantai Yang, and Jianping Deng*

State Key Laboratory of Chemical Resource Engineering, College of Materials Science and Engineering, Beijing University of Chemical Technology, Beijing 100029, China

Supporting Information

ABSTRACT: This article reports an original, versatile strategy to chirally functionalize graphene oxide (GO) with optically active helical-substituted polyacetylene. GO was first converted into alkynyl-GO containing polymerizable −C≡C moieties, which took part in the polymerization of another chiral acetylenic monomer, yielding the expected GO hybrid covalently grafted with chiral helical polyacetylene chains. Transmission electron microscopy, atomic force microscopy, X-ray diffraction, Fourier transform infrared spectroscopy, Raman spectroscopy, X-ray photoelectron spectroscopy, and thermogravimetric analyses verified the successful attachment of substituted polyacetylene chains on GO by covalent chemical bonding. Moreover, circular dichroism effects and UV−vis absorption demonstrated that the GO hybrid possessed fascinating optical activity. It also largely improved the dispersibility of GO in tetrahydrofuran. The GO-derived hybrid was further used as a chiral inducer toward enantioselective crystallization of alanine enantiomers. L-Alanine was preferably induced to crystallize, forming rodlike crystals.

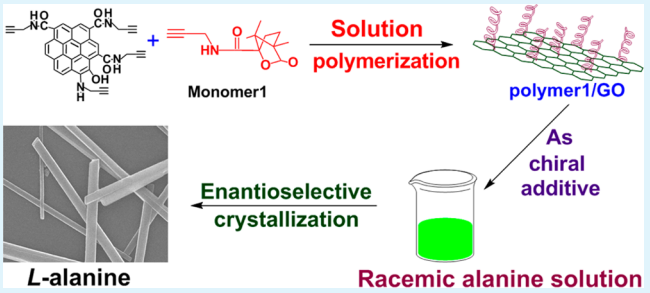

KEYWORDS: *chiral functionalization, enantioselective crystallization, graphene oxide, helical polymer, optical activity*

1. INTRODUCTION

Graphene and its derivatives, as novel materials consisting of one-atom-thick planar layers composed of sp^2-hybridized carbon structure, have gathered ever-increasing interest in the field of materials science because of their remarkable physicochemical properties.[1,2] Some interesting properties of graphene include high specific surface area, extraordinary electronic properties, high mechanical strength, and superior thermal and electrical conductivities.[3−6] Graphene oxide (GO) also evokes enormous attention as an important branch of graphene[7] because of its low cost and large-scale production, together with satisfactory dispersibility in organic solvents.[8,9] GO can also serves as a precursor for the preparation of reduced GO (RGO). More remarkably, a variety of oxygen-containing organic moieties like carboxyl, hydroxyl, and epoxy groups exist in GO sheets. These reactive groups enable GO to be highly attractive for further functionalization and for the development of novel advanced materials.[10−18] The generally used materials for functionalizing GO range from small organic molecules[19−22] to (bio)macromolecules.[23−26] However, chiral (macro)molecules, even though they have formed a significant research area, have been seldom utilized to functionalize GO. We reason that the practices along this direction will undoubtedly lead to enormous novel materials, in particular intriguing chiral materials. Even though only a few chiral compounds have been attached to graphene (including GO and RGO), the resulting chiral hybrids have demonstrated promises in asymmetric catalysis,[27] chiral recognition/adsorption,[28−30] and chiral sensoring.[31] The studies also open up new applications of graphene materials and are expected to promote advancements in chiral-related technologies. The present article reports a novel type of chirally functionalized GO hybrids and their interesting application in enantioselective crystallization.

The importance of chiral (macro)molecules has been extensively recognized, well exemplified by chiral drugs. Chiral helical polymers are particularly interesting because of the well-known "chiral amplification" effects.[32,33] In spite of the various artificial chirally helical polymers already prepared,[34−41] so far their functionalization of GO has not yet been explored. The major reason for this issue may be due to the lack of an easy methodology by which to efficiently attach helical polymers on GO sheets. In our earlier studies, we prepared a series of optically active helical polyacetylenes and nano- and micro-particles thereof.[42−44] More recently, we succeeded in immobilizing chiral helical polyacetylenes on RGO through $\pi-\pi$ stacking.[45] The as-obtained RGO hybrid demonstrated the desirable optical activity. Apart from noncovalent $\pi-\pi$ stacking, we also immobilized helical polyacetylene-based nanoparticles

Received: April 11, 2014
Accepted: June 5, 2014
Published: June 5, 2014

 © 2014 American Chemical Society dx.doi.org/10.1021/am502194b | ACS Appl. Mater. Interfaces 2014, 6, 9790−9798

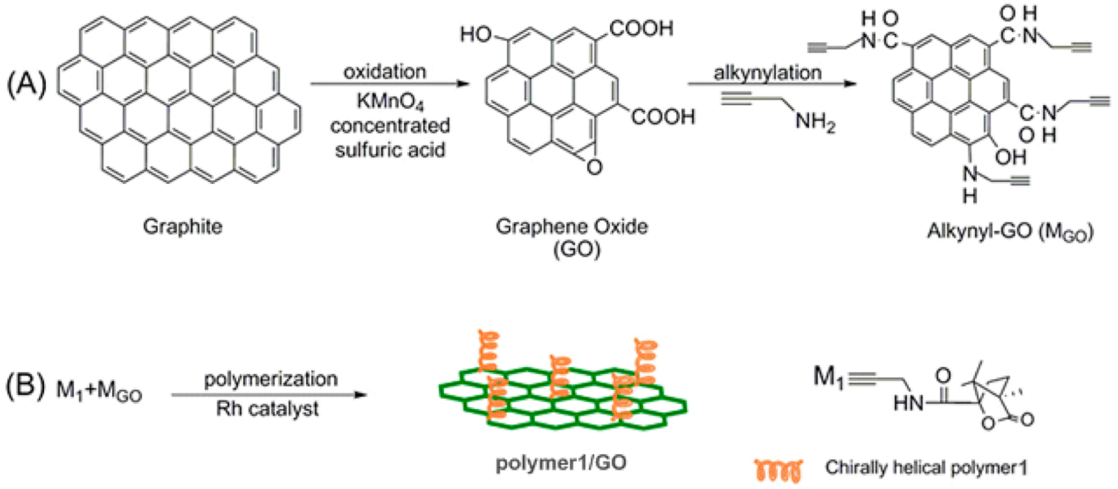

Figure 1. Illustration for the preparation of alkynyl-GO and polymer1/GO.

on GO sheets through covalently chemical bonds. The functionalized GO hybrids also demonstrated intriguing optical activity and especially their potential in enantioselective crystallization.[46] We further envision that direct grafting of helical polymer chains by chemical bonds onto GO shall be more straightforward and attractive in the construction of intriguing chiral GO materials. Accordingly, in the present study, we made specific efforts along this direction and successfully grafted optically active helical polyacetylene chains on GO. Remarkably, such chiral GO hybrids also induced enantioselective crystallization[47] by utilizing alanine enantiomers as the model of chiral compounds. Compared to earlier strategies,[46] the present one is more advantageous because of the easy process for chiral functionalization of GO and because the helical polymer chains are grafted more firmly onto GO relative to the physically $\pi-\pi$-stacking manner.[45] Beyond the success in the preparation of a novel type of GO-based chiral hybrid materials, the present methodology can be taken as a robust platform for establishing more advanced materials, especially chiral materials derived from GO.

2. EXPERIMENTAL SECTION

2.1. Materials. (nbd)$Rh^+B^-(C_6H_5)_4$[48] and monomer (M1)[49] were prepared according to earlier reports. Propargylamine, isobutyl chloroformate, *N*-methylmorpholine, dicyclohexyl carbodiimide, 4-(dimethylamino)pyridine, and alanines were used as obtained from Aldrich. Graphite powder was bought from Alfa Aesar, and the parameters for it are 300 mesh, carbon content 75−82%, and ash 18−25%. A hydrogen peroxide solution (H_2O_2, 30%), potassium permanganate ($KMnO_4$), HCl, H_2SO_4, NaOH, *N*,*N*′-dimethylformamide (DMF), and tetrahydrofuran (THF) were used as received from Beijing Chemical Company.

2.2. Measurements. General characterizations were carried out in the same way as those in earlier reports.[45,46] Atomic force microscopy (AFM) images were viewed by Veeco DI instrument.

2.3. Preparation of Graphene Oxide (GO) and Alkynyl-GO. GO was prepared from natural graphite powder based on the method of Hummers and Offemann.[50] Detailed processes were described in our earlier report.[46] Alkynylation of GO was also accomplished by using the same method in the previous article.[46]

2.4. Preparation of GO Hybrid (polymer1/GO). Figure 1 presents the preparation of functionalized GO by covalent bonding of polymer chains (denoted as polymer1) from monomer M1 onto GO, to form polymer1/GO hybrid via a solution polymerization approach. The underlying concept is designed by referring to our previous investigations for the preparation of chiral helical polyacetylene by solution polymerization.[45,49] The major preparation procedure is stated below. First, alkynyl-GO (0.05 g) was dispersed under sonication in a 100 mL round-bottomed flask containing DMF (30 mL). The process of sonication lasted for about 90 min to achieve a homogeneous dispersion of alkynyl-GO in DMF. Then a hydrophobic rhodium catalyst (nbd)$Rh^+B^-(C_6H_5)_4$ (0.0011 g) solution (DMF, 1 mL) was added dropwise to the above dispersion to initiate the solution polymerization of M1 (0.5 g). In the course of polymerization of M1, the −C≡C groups in alkynyl-GO also underwent polymerization, by which the in situ formed polymer chains are covalently grafted onto GO sheets. The solution polymerization proceeded under N_2 and continued at 30 °C for 5 h. The resulting polymer solution was centrifuged at 20000 rpm for 20 min, providing polymer1/GO hybrid. The product was further washed with THF at least four times and finally dried in vacuum.

2.5. Enantioselective Crystallization. The above-obtained polymer1/GO was used as a chiral additive to perform enantioselective crystallization with D- and L-alanine as the models for chiral compounds. A total of 3.5 mg of polymer1/GO was added in a supersaturated racemic alanine aqueous solution (0.1 g/mL, 30 °C) and stirred for 30 min. The alanine mixture was then placed in a refrigerator (approximately 2 °C) for cooling. A total of 3 days later, the crystals of alanine were taken out, dried under ambient conditions, and then subjected to characterization.

3. RESULTS AND DISCUSSION

3.1. Strategy for the Fabrication of polymer1/GO. In the present study, we prepared a novel GO hybrid covalently grafted with optically active helical polyacetylene through a solution polymerization route. Our major purposes are (1) to chirally functionalize GO with helical polymer chains (polymer1, derived from monomer M1), aimed at affording GO hybrid with fascinating optical activity, (2) to enhance the dispersibility of GO in organic solvents due to the presence of hydrophobic polymer chains, and (3) to create a distinctive methodology for the preparation of novel hybrid materials constructed by GO and synthetic polymers. The strategy for the preparation of the hybrid material is illustratively presented in Figure 1.

The procedure majorly includes two processes. In the first one (A, in Figure 1), GO was prepared from graphite by using the Hummers technique with little modification. GO was alkynylated to produce alkynyl-GO. This process was performed by reactions between the −COOH functional groups (and epoxy groups) on GO with the amino group in propargylamine. The target is to graft polymerizable −C≡C

dx.doi.org/10.1021/am502194b | ACS Appl. Mater. Interfaces 2014, 6, 9790−9798

units on GO via chemical bonding, yielding alkynyl-GO. In the second process (B, in Figure 1), substituted acetylene M1 underwent catalytic polymerization initiated by a rhodium-derived catalyst. Meanwhile, the polymerizable −C≡C units on GO sheets also participated in the polymerization of M1. This practice led to GO-hybrid-containing polymer chains. The facile and meanwhile efficient strategy resulted in the expected polymer1/GO hybrid. As a new chiral GO material, polymer1/GO remarkably integrated GO and helical polyacetylene chains (majorly derived from monomer M1). As expected, the helical polymer chains facilitated GO to demonstrate optical activity, and meanwhile the polymer chains helped to improve the dispersibility of GO in THF, as will be discussed in detail later.

Herein it should be pointed out that there have already been a number of studies in the literature dealing with attaching synthetic polymer chains onto GO. This can be achieved by noncovalent interactions,[51−53] Click reactions,[54−56] and specific chemical reactions[57,58] or with GO derivative as the initiator, leading to polymerizations.[59] However, the present study provided a distinctive approach; i.e., alkynyl-GO practically acted as a comonomer, as illustratively presented in Figure 1.

3.2. Fourier Transorm Infrared (FT-IR) Spectra. To verify the successful fabrication of a GO-based hybrid, namely, polymer1/GO, the product obtained after polymerization was first characterized by FT-IR spectroscopy. The obtained FT-IR spectra are presented in Figure 2.

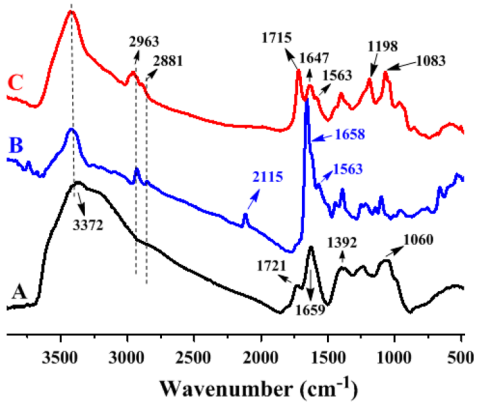

Figure 2. FT-IR spectra for (A) GO, (B) alkynyl-GO, and (C) polymer1/GO (measured in the form of KBr disks).

In the spectrum of the initial GO (spectrum A, Figure 2), peaks appeared at 1060 cm^{-1} (C−O stretching, epoxy), 1392 cm^{-1} (−OH stretching, carboxylic acid), 1659 cm^{-1} (C═C skeletal vibrations, unoxidized graphite domains), and 1721 and 3372 cm^{-1} (C═O and −OH, carboxylic acid). After alkynylation, new peaks can be observed in alkynyl-GO (Figure 2, B). The peak located at 2115 cm^{-1} reflects the −C≡C moieties. The peaks at 1563 and 1658 cm^{-1} reflect [−C(O)-NH−] the amide structure and further confirm the formation of an amide bond through the alkynylation process of GO. In addition, methylene ($-CH_2-$) stretching vibrations at 2963 and 2881 cm^{-1} are also observed in alkynyl-GO. Spectrum C shows that the original peak (2115 cm^{-1}, reflecting the C≡C group, spectrum B) disappeared, clarifying that both the −C≡C units in M1 and those on alkynyl-GO were polymerized. In addition, the two peaks at 1198 and 1083 cm^{-1} (spectrum C) indicate C−O stretching in polymer1 and GO. Accordingly, the FT-IR spectral analyses above verify the efficient polymerization of M1 and the formation of polymer1/GO hybrid.

3.3. Transmission Electron Microscopy (TEM) Images. The FT-IR spectra discussed above just preliminarily confirm that monomer M1 underwent polymerization and polymer1/GO was fabricated. Nevertheless, more characterizations are still required to justify the successful formation of the polymer1/GO hybrid. Hence, a TEM technique was utilized to observe the difference in morphology between GO and GO hybrid (polymer1/GO). For observation of TEM, GO and polymer1/GO were separately dispersed in THF under sonication. Then the dispersions were placed on a carbon grid (200 mesh) and viewed by a TEM microscope. The recorded TEM images are presented in Figure 3A,B.

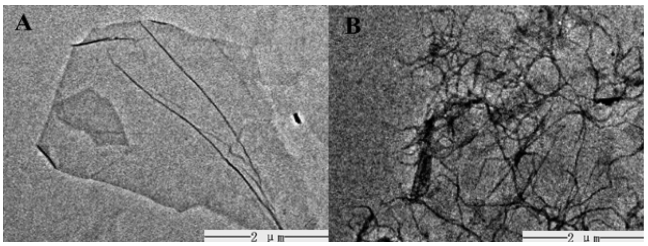

Figure 3. Typical TEM images of pristine GO (A) and polymer1/GO (B).

As observed in Figure 3A, pristine GO showed a rather smooth morphology; however, the layered structure led to the formation of wrinkles. Figure 3B presents the TEM image of the as-prepared polymer1/GO hybrid, according to the strategy illustrated in Figure 1. A large number of wrinkles appeared in the GO hybrid. When a comparison is made between the two TEM images in Figure 3, we can clearly see that the number of wrinkles drastically increased in the GO hybrid. The appearance of such remarkable wrinkles is attributed to the enhanced interactions between graphene layers due to the polymer1 chains derived from M1. The increased wrinkles on GO sheets may be desirable in terms of practical applications.[60]

AFM images of alkynyl-GO and polymer1/GO hybrid were also observed, as illustrated in Figure 4A,B. For AFM measurement, alkynyl-GO and polymer1/GO were separately dispersed in ethanol and then deposited on a silicon wafer. The

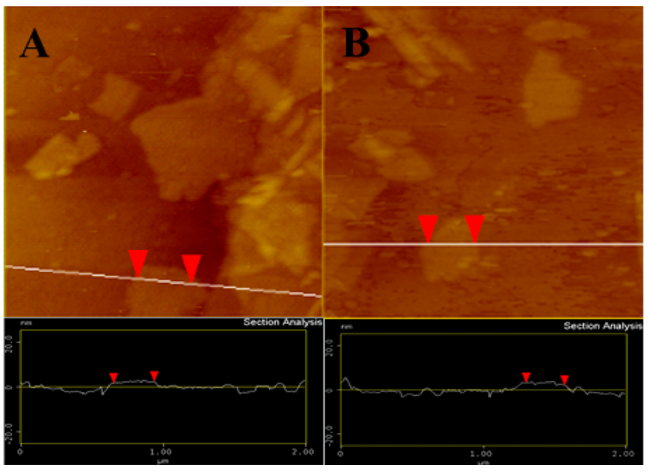

Figure 4. Typical AFM images of pristine alkynyl-GO (A) and polymer1/GO (B).

dx.doi.org/10.1021/am502194b | ACS Appl. Mater. Interfaces 2014, 6, 9790−9798

AFM images show that the height of the pristine alkynyl-GO surface was 0.784 nm, while it was 1.446 nm for polymer1/GO hybrid. This further indicates that the substituted polyacetylene chains were attached to GO sheets.

The presence of polymer chains helped improve GO's dispersibility in solvents, for instance, THF, as depicted in Figure 5. Figure 5A shows that, even in the absence of a specific dispersant, polymer1/GO became smoothly dispersible in THF. More remarkably, the resulting dispersion could remain stable, and no obvious precipitation occurred even after storage under ambient conditions for more than 1 month (Figure 5B). Although GO also became dispersible in THF (Figure 5C), nonetheless, obvious precipitation took place after storage for just 3 h, as demonstrated in Figure 5D. On the basis of investigations, it is reasonable to conclude that we created a facile yet powerful methodology to graft helical polyacetylene chains onto GO sheets. Furthermore, the grafted polymer chains largely improved the stability of the dispersion of GO hybrid in THF. More interestingly, the grafted polymers also afforded GO with fascinating optical activity, as will be reported next.

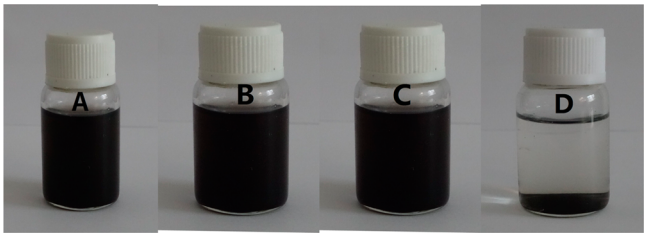

Figure 5. polymer1/GO (A and B) and pristine GO (C and D) dispersed in THF (room temperature): (A and C) original dispersions; (B and D) dispersions kept for more than 30 days (B) and 3 h (D). All of the spectra were recorded at room temperature.

3.4. Circular Dichroism (CD) and UV−Vis Absorption Spectra. The primary objective of the present study is to functionalize GO with optically active helical polyacetylene chains (polymer1), by which to render GO with optical activity. Taking into consideration the significant importance of chiral materials, particularly in pharmaceutics and biology, a judicious association of chiral molecules with GO, in principle, will create a great number of advanced functional materials. To confirm that polymer1/GO possessed optical activity, polymer1/GO hybrid dispersion in THF was subjected to characterization by CD and UV−vis spectroscopy, which were widely used in our previous studies dealing with helical polymers.[42−45,61] The recorded CD and UV−vis absorption spectra are displayed in Figure 6A,B.

The dispersion performed intense CD effects and strong UV−vis absorption both at about 340 nm. Next, to further elucidate the observed CD effect and UV−vis absorption, we specifically polymerized M1 by using THF as the solvent under identical conditions but without alkynyl-GO, by using the earlier method dealing with solution polymerization of substituted acetylenes.[45,49] The recorded CD and UV−vis absorption spectra of homopolymer1 (the homopolymer from M1) are also shown in Figure 6A,B. For homopolymer1, a strong CD signal and a UV−vis absorption peak also appeared around 340 nm. Referring to our previous studies,[42−45,61,62] the observed CD signals and UV−vis absorptions located at 340 nm (in both homopolymer1 and polymer1/GO hybrid) are ascribed to polymer1 chains adopting helical structures. In more detail, the earlier studies demonstrated that when substituted polyacetylenes adopted helical conformations with predominant helicity, they always showed CD effects and UV−vis absorptions at a wavelength ranging from 320 to 450 nm.[42−45] On the basis of Figure 6, we deduced that polymer1 chains covalently grafted on GO took helical structures with one predominant helicity. This feature causes the hybrid polymer1/GO to demonstrate intriguing optical activity.

Next, we specifically manifested that CD and UV−vis absorption performed in polymer1/GO (Figure 6) originated in the polymer chains grafted on GO through chemical bonds. To achieve this goal, a pure polymer1/GO hybrid should be produced first. Thus, the obtained polymer1/GO hybrid was dispersed in THF, which was then isolated by centrifugation of 20000 rpm for 20 min. Theoretically, the polymer chains derived from M1, if they are not grafted onto GO by chemical bonds, will be dissolved in THF because of their good solubility. After centrifugation at a high speed, such free polymer chains should be separated from GO. On the other hand, the C≡C units preattached to GO shall copolymerize with M1. Such a process will lead to copolymer chains that cannot be removed by simple physical means. According to the analyses above, we convincingly verified that polymer1 chains

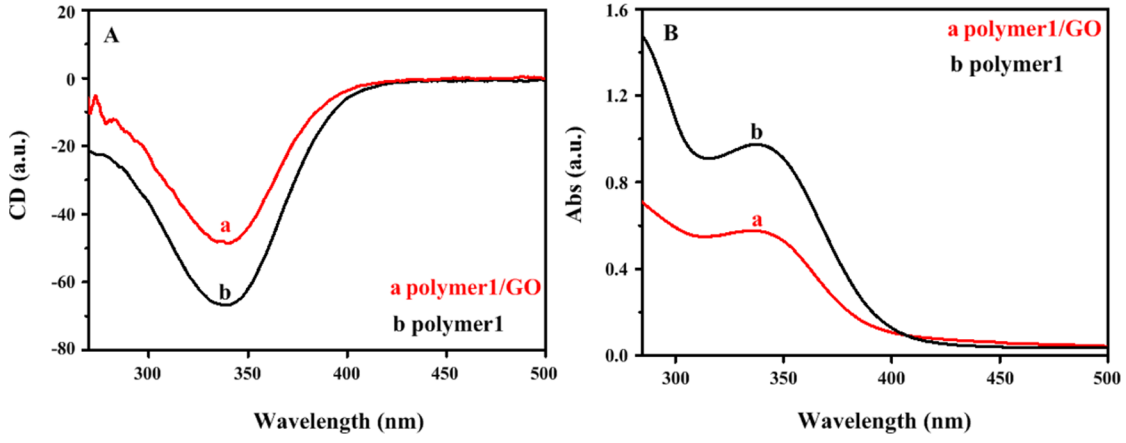

Figure 6. CD (A) and UV−vis absorption (B) spectra recorded in a polymer1/GO dispersion and a homopolymer1 solution (in THF). For homopolymer1 in a THF solution, M_n = 8000 and M_w/M_n = 2.1. The spectra were recorded at room temperature.

dx.doi.org/10.1021/am502194b | ACS Appl. Mater. Interfaces 2014, 6, 9790−9798

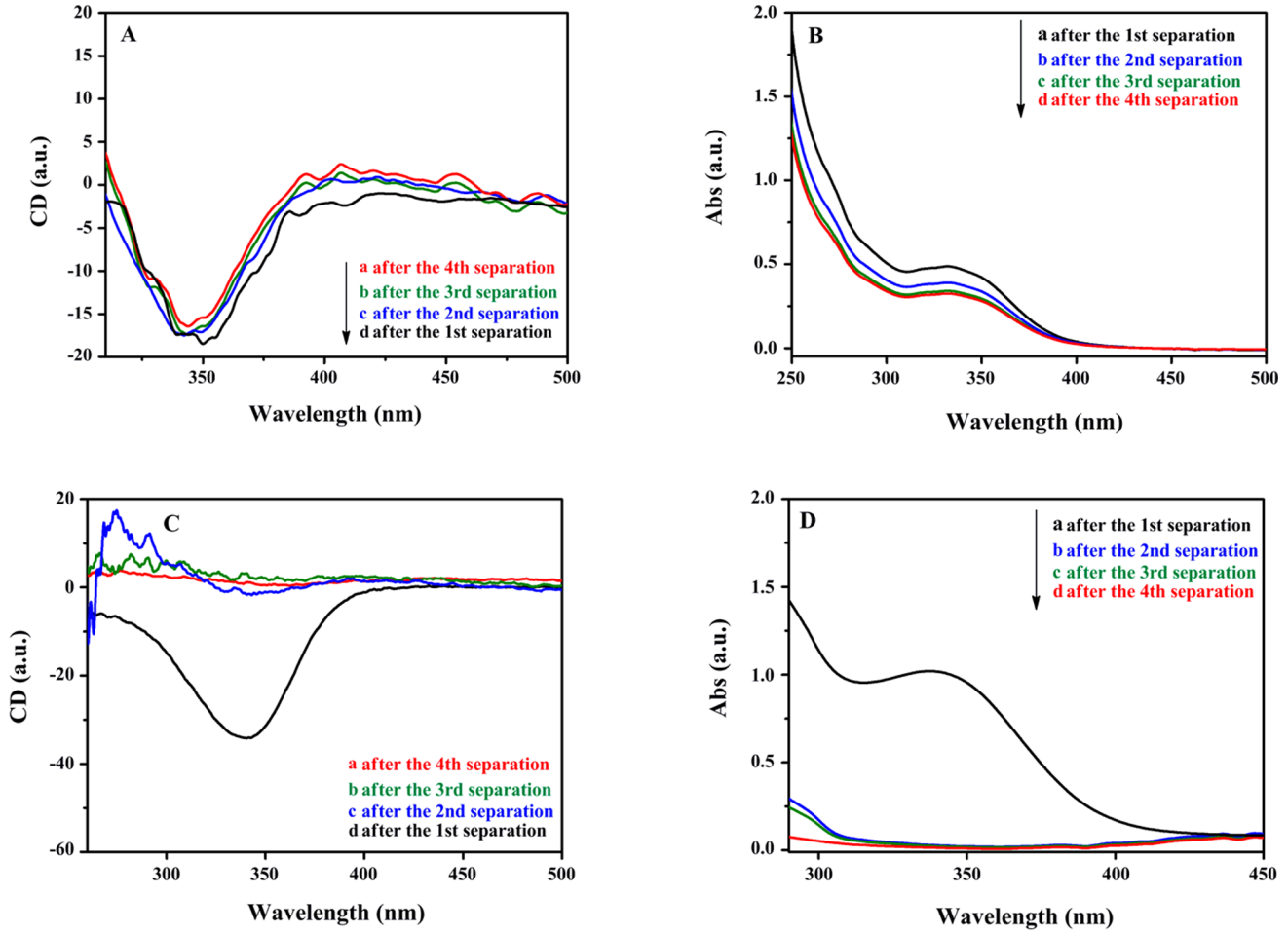

Figure 7. Typical CD (A) and UV−vis absorption (B) spectra recorded in a polymer1/GO dispersion and a homopolymer1 solution (in THF). For homopolymer1 in a THF solution, M_n = 8000 and M_w/M_n = 2.1. The spectra were recorded at room temperature.

were attached to GO actually by means of chemical bonding, as demonstrated in Figure 7.

The prepared polymer1/GO was washed by THF and then centrifuged to offer a pure GO hybrid. After each cycle of washing with THF, the purified GO hybrid sample and corresponding THF solution were characterized by CD and UV−vis spectra. Herein the purification process was repeated a total of four times. The relevant CD effects and UV−vis absorptions are illustrated in Figure 7. After the first cycle of purification, the polymer1/GO sample showed pronounced CD effects and strong UV−vis absorption around 340 nm (Figure 7A,B), but for the corresponding THF filtrate, an intense CD signal and strong UV−vis absorption peaks were also observed (Figure 7C,D). Parts C and D of Figure 7 demonstrate that a certain amount of polymer1 was dissolved in a THF solution, also reflecting that part of polymer1 was just physically attached to GO sheets.

When polymer1/GO hybrid was purified by using THF two to four times, the related CD signals and UV−vis absorptions (Figure 7A,B) were still strong; more exactly, the intensity of the CD effects and UV−vis absorptions changed little. However, the THF solutions (Figure 7C,D) showed no CD and UV−vis absorption at wavelengths between 300 and 400 nm. The observations in Figure 7, together with the CD and UV−vis spectra presented in Figure 6 and the TEM images (Figure 3), convincingly demonstrate that polymer1/GO was successfully prepared, in which the polymer chains were grafted onto GO sheets by chemical bonds.

3.5. X-ray Photoelectron Spectroscopy (XPS) Spectra. To explore the obtained polymer1/GO further, we subsequently performed XPS characterization. The obtained spectra are displayed in Figure S1 (Supporting Information). Before measurement, all of the samples were purified by an excessive amount of THF, dried, and then subjected to XPS measurement. Figure S1 in the SI shows a clear comparison among GO, alkynyl-GO, and polymer1/GO hybrid. For the original GO, a nitrogen element was not detected; however, alkynyl-GO exhibited a peak (406 eV), reflecting the presence of a nitrogen element in the sample. In more detail, the nitrogen content was determined to be 0.68%. For polymer1/GO, a drastic increase in the nitrogen element to 4.96% was observed because of the polymer chains derived from M1. The XPS spectra and other characterizations show that a noticeable amount of polymer1 was grafted onto GO sheets.

3.6. X-ray Diffraction (XRD) Pattern. XRD is another widely used technique to characterize GO and its derivatives. XRD was utilized to determine the spacing between GO layers before and after functionalization. The recorded XRD patterns are presented in Figure 8. For GO, an intense peak (2θ = 10.41°) appears in the XRD pattern, indicating that d (the interlayer distance) was ca. 0.85 nm, well in accordance with the earlier report.[45] For alkynyl-GO and polymer1/GO, one peak (001) with a lower value (2θ = 10.07 or 9.73°) can be

dx.doi.org/10.1021/am502194b | ACS Appl. Mater. Interfaces 2014, 6, 9790−9798

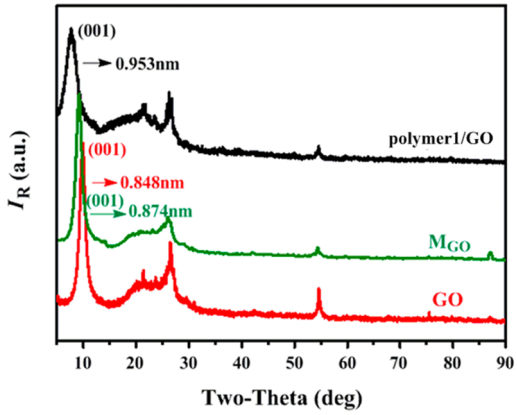

Figure 8. XRD pattern of pristine GO, alkynyl-GO (M_{GO}), and GO hybrid.

seen in Figure 8. This indicates that the interlayer spacing in GO hybrid is slightly enhanced (d of approximately 0.88 and 0.95 nm, respectively) relative to pristine GO. It should be pointed out that, for all of the samples, a peak appeared at 2θ = 27−28°. This indicates that graphite was incompletely oxidized in the study.

3.7. Raman Spectra. With Raman spectroscopy, we can determine the ID/IG ratio of GO.[63] ID means the peak intensity at ∼1347 cm^{-1}, while IG indicates the peak intensity at 1586 cm^{-1}. They respectively correspond to the number of sp^3 and sp^2 carbon atoms. The recorded Raman spectra are presented in Figure 9. We see that the ratio of ID/IG enhanced

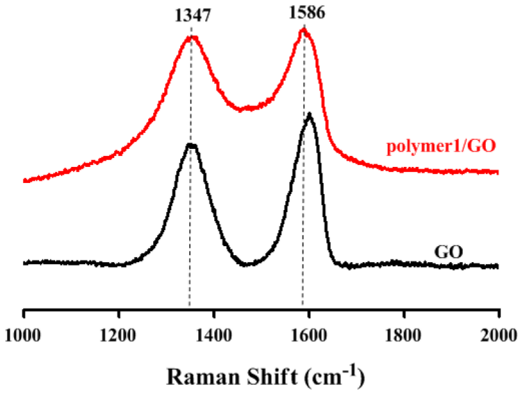

Figure 9. Raman spectra of GO and polymer1/GO.

from 0.83 (for GO) to 1.21 (for polymer1/GO hybrid). The enhancement in ID/IG indicates a noticeable reduction in the average size of sp^2 domains in the functionalized GO.[64] Raman spectral analyses also provide further support for our conclusion that helical polymer1 was grafted covalently onto GO sheets.

3.8. Thermogravimetric Analysis (TGA). A TGA technique was taken to assess the stability of polymer1/GO hybrid against heat. TGA measurement was performed from room temperature to 800 °C (at 10 °C/min) under N_2. To make a vivid comparison, pristine GO and polymer1 (polymer from M1) were also examined by TGA. The data are displayed in Figure 10. For GO, the oxygen-containing groups on the GO surface started to burn at about 190 °C because of the reactive small-molecule organic structures (−COOH, −OH, etc.). polymer1 remained stable at this temperature, as seen from

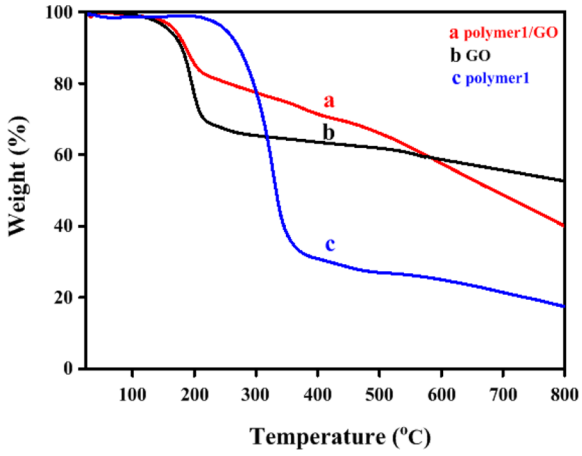

Figure 10. TGA curves of (a) polymer1/GO, (b) GO, and (c) polymer1. Analyses were carried out at a rate of 10 °C/min under N_2.

the curve. For polymer1/GO, a minor improvement is observed in the TGA curve. This is due to the fact that a majority of the initial small-molecule organic groups had been transformed to polymer chains during the formation of GO hybrid. The residual nonvolatile materials remained stable up to 800 °C. Hybrid polymer1/GO lost approximately 18.5 wt % when the temperature was elevated from 250 to 475 °C, further showing about 18.5 wt % of polymer1 grafted onto GO sheets.

3.9. Enantioselective Crystallization. The thus-prepared chiral GO hybrids potentially possess important applications, in particular as chiral materials. To justify our anticipation, we utilized the polymer1/GO hybrid prepared above as a specific chiral inducer to conduct enantioselective crystallization[65,66] of alanine enantiomers, which were taken as model chiral compounds. We found that L-alanine was predominantly induced to crystallize to form rodlike crystals, as presented in Figure 11A. The enantiomeric excess of the induced crystals was 73%. The detailed CD spectra and XRD patterns of the induced crystals are presented in Figures S2 and S3 in the SI. A combination of the CD effects and XRD patterns demonstrates that L-alanine rather than D-alanine was preferentially induced to crystallize. In the cases without the addition of an additive (Figure 11B) and with alkynyl-GO as the additive (Figure 11C), only disordered crystals were formed. This observation is in well accordance with our earlier study, in which polymer particles with optical activity were immobilized on GO and subsequently employed as special chiral selectors for enantioselective crystallization.[46] This further indicates that, even though the optically active helical polyacetylene was supported on GO sheets in varied forms, i.e., free chains and solid particles, it preferentially induced an alanine enantiomer of the same chirality (L-alanine) to crystallize, and, moreover, the induced crystals formed the same morphology (rodlike crystals). The mechanism for enantioselective crystallization is briefly stated herein. The chiral GO hybrid acted as a special chiral additive. At the beginning of crystallization of alanine, L-alanine was preferably adsorbed on the chiral GO hybrid because of the chirally helical polyacetylene chains. The chiral hybrid with L-alanine further served as a nucleation site for subsequent enantioselective crystallization of more alanine. Unfortunately, because the other enantiomer for preparing M1 (Figure 1) is unavailable, we could not further explore in depth the effects of the helicity of polymer1 on enantioselective crystallization. It should be noted that, compared to the earlier

dx.doi.org/10.1021/am502194b | ACS Appl. Mater. Interfaces 2014, 6, 9790−9798

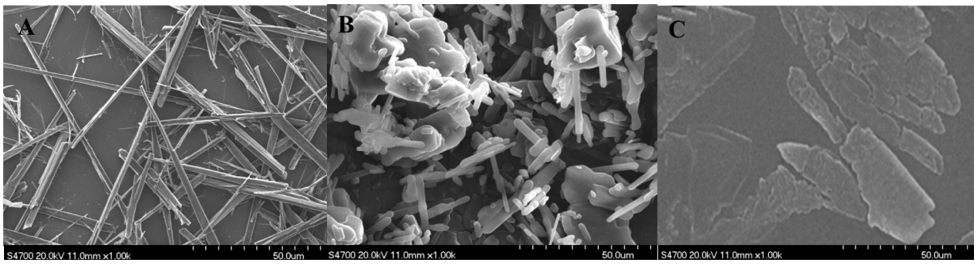

Figure 11. Typical SEM images of the crystals majorly formed by L-alanine via enantioselective crystallization with polymer1/GO hybrid (A) and crystals formed without additive (B) and with alkynyl-GO as the additive (C).

strategy,[46] the present one is more straightforward for preparing chirally functionalized GO.

4. CONCLUSIONS

We prepared novel GO hybrid materials by covalently functionalizing GO using chirally helical polyacetylene, which rendered GO with remarkable chirality. Additionally, the substituted polyacetylene chains also enabled GO hybrid to be dispersible in THF. GO hybrids were produced by polymerization of a chiral acetylene monomer in solution, in the presence of alkynyl-GO as an actual comonomer. Namely, the reactive C≡C bonds on GO participated in the polymerization, resulting in polymer chains of monomer M1 covalently attached to GO sheets. The resulting chiral GO hybrid preferentially induced L-alanine to form crystals from the racemic solution under the investigated conditions. The present methodology is facile and powerful for functionalization of GO, being applicable not only to acetylenics but also to other types of polymers. This versatile platform is expected to lead to a great variety of novel GO-derived advanced chiral materials. The judicious combination of chiral polymers with GO hopefully leads to new asymmetric catalysts, chiral sensors, chiral adsorbents, etc. We are currently continuing our efforts along these directions.

■ ASSOCIATED CONTENT

Supporting Information

XPS spectrum of polymer 1/GO and CD spectra and XRD patterns of the L-alanine crystals obtained through enantioselective crystallization. This material is available free of charge via the Internet at http://pubs.acs.org.

■ AUTHOR INFORMATION

Corresponding Author

*Tel: +86-10-6443-5128. Fax: +86-10-6443-5128. E-mail: dengjp@mail.buct.edu.cn.

Notes

The authors declare no competing financial interest.

■ ACKNOWLEDGMENTS

This work was supported by the National Natural Science Foundation of China (Grants 21274008 and 21174010), the Funds for Creative Research Groups of China (Grant 51221002), and the "Specialized Research Fund for the Doctoral Program of Higher Education" (SRFDP Grant 20120010130002).

■ REFERENCES

(1) Novoselov, K. S.; Geim, A. K.; Mozorov, S. V.; Jiang, D.; Zhang, Y.; Dubonos, S. V.; Grigorieva, I. V.; Firsov, A. A. Electric Field Effect in Atomically Thin Carbon Films. *Science* **2004**, *306*, 666−669.

(2) Lee, C.; Wei, X. D.; Kyser, J. W.; Hone, J. Measurement of the Elastic Properties and Intrinsic Strength of Monolayer Graphene. *Science* **2008**, *321*, 385−388.

(3) Choi, S.-J.; Jang, B.-H.; Lee, S.-J.; Min, B. K.; Rothschild, A.; Kim, I.-D. Selective Detection of Acetone and Hydrogen Sulfide for the Diagnosis of Diabetes and Halitosis Using SnO_2 Nanofibers Functionalized with Reduced Graphene Oxide Nanosheets. *ACS Appl. Mater. Interfaces* **2014**, *6*, 2588−2597.

(4) Rumyantsev, S.; Liu, G.; Shur, M. S.; Potyrailo, R. A.; Balandin, A. A. Selective Gas Sensing with a Single Pristine Graphene Transistor. *Nano Lett.* **2012**, *12*, 2294−2298.

(5) Miller, J. R.; Outlaw, R. A.; Holloway, B. C. Graphene Double-Layer Capacitor with AC Line-Filtering Performance. *Science* **2010**, *329*, 1637−1639.

(6) Kemp, K. C.; Seema, H.; Saleh, M.; Le, N. J.; Mahesh, K.; Chandra, V.; Kim, K. S. Environmental Applications Using Graphene Composites: Water Remediation and Gas Adsorption. *Nanoscale* **2013**, *5*, 3149−3171.

(7) Li, X.; Cai, W.; An, J.; Kim, S.; Nah, J.; Yang, D.; Piner, R.; Velamakanai, A.; Jung, I.; Tutuc, E.; Banerjee, S. K.; Colombo, L.; Ruoff, R. S. Large-Area Synthesis of High-Quality and Uniform Graphene Films on Copper Foils. *Science* **2009**, *324*, 1312−1314.

(8) Yan, L.; Zheng, Y. B.; Zhao, F.; Li, S.; Gao, X.; Xu, B.; Weiss, P. S.; Zhao, Y. Chemistry and Physics of a Single Atomic Layer: Strategies and Challenges for Functionalization of Graphene and Graphene Based Materials. *Chem. Soc. Rev.* **2012**, *41*, 97−114.

(9) Chen, D.; Tang, L.; Li, J. Graphene-Based Materials in Electrochemistry. *Chem. Soc. Rev.* **2010**, *39*, 3157−3180.

(10) Collins, W. R.; Lewandowski, W.; Schmois, E.; Walish, J.; Swager, T. M. Claisen Rearrangement of Graphite Oxide: A Route to Covalently Functionalized Graphenes. *Angew. Chem., Int. Ed.* **2011**, *50*, 8848−8852.

(11) Collins, W. R.; Schmois, E.; Swager, T. M. Graphene Oxide as an Electrophile for Carbon Nucleophiles. *Chem. Commun.* **2011**, *47*, 8790−8792.

(12) Das, S. K.; KC, C. B.; Ohkubo, K.; Yamada, Y.; Fukuzumi, S.; D'Souza, F. Decorating Single Layer Graphene Oxide with Electron Donor and Acceptor Molecules for the Study of Photoinduced Electron Transfer. *Chem. Commun.* **2013**, *49*, 2013−2015.

(13) Feng, L.; Wu, L.; Qu, X. New Horizons for Diagnostics and Therapeutic Applications of Graphene and Graphene Oxide. *Adv. Mater.* **2013**, *25*, 168−186.

(14) He, F.; Fan, J.; Ma, D.; Zhang, L.; Leung, C.; Chan, H. L. The Attachment of Fe_3O_4 Nanoparticles to Graphene Oxide by Covalent Bonding. *Carbon* **2010**, *48*, 3139−3144.

(15) Feng, R.; Zhou, W.; Guan, G.; Li, C.; Zhang, D.; Xiao, Y.; Zheng, L.; Zhu, W. Surface Decoration of Graphene by Grafting Polymerization Using Graphene Oxide as the Initiator. *J. Mater. Chem.* **2012**, *22*, 3982−3989.

(16) Jiang, K.; Ye, C.; Zhang, P.; Wang, X.; Zhao, Y. One-Pot Controlled Synthesis of Homopolymers and Diblock Copolymers

Grafted Graphene Oxide Using Couplable RAFT Agents. *Macromolecules* **2012**, *45*, 1346−1353.
(17) Badri, A.; Whittaker, M. R.; Zetterlund, P. B. Modification of Graphene/Graphene Oxide with Polymer Brushes Using Controlled/Living Radical Polymerization. *J. Polym. Sci., Part A: Polym. Chem.* **2012**, *50*, 2981−2992.
(18) Kuila, T.; Bose, S.; Mishra, A. K.; Khanra, P.; Kim, N. H.; Lee, J. H. Chemical Functionalization of Graphene and Its Applications. *Prog. Polym. Sci.* **2012**, *57*, 1061−1105.
(19) Ogoshi, T.; Ichihara, Y.; Yamagishi, T.; Nakamoto, Y. Supramolecular Polymer Networks from Hybrid between Graphene Oxide and Per-6-Amino-β-Cyclodextrin. *Chem. Commun.* **2010**, *46*, 6087−6089.
(20) Herrera-Alonso, M.; Abdala, A. A.; McAllister, M. J.; Aksay, I. A.; Prud'homme, R. K. Intercalation and Stitching of Graphite Oxide with Diaminoalkanes. *Langmuir* **2007**, *23*, 10644−10649.
(21) Dey, R. S.; Raj, C. R. Redox-Functionalized Graphene Oxide Architecture for the Development of Amperometric Biosensing Platform. *ACS Appl. Mater. Interfaces* **2013**, *5*, 4791−4798.
(22) Mondal, A.; Jana, N. R. Fluorescent Detection of Cholesterol Using β-Cyclodextrin Functionalized Graphene. *Chem. Commun.* **2012**, *48*, 7316−7318.
(23) Jin, L.; Yang, K.; Yao, K.; Zhang, S.; Tao, H.; Lee, S.-T.; Liu, Z.; Peng, R. Functionalized Graphene Oxide in Enzyme Engineering: A Selective Modulator for Enzyme Activity and Thermostability. *ACS Nano* **2012**, *6*, 4864−4875.
(24) Beckert, F.; Friedrich, C. C.; Thomann, R.; Mülhaupt, R. Sulfur-Functionalized Graphene as Macro-Chain-Transfer and RAFT Agents for Producing Graphene Polymer Brushes and Polystyrene Nanocomposites. *Macromolecules* **2012**, *45*, 7083−7090.
(25) Saxena, A. P.; Deepa, M.; Joshi, A. G.; Bhandari, S.; Srivastava, A. K. Poly(3,4-ethylenedioxythiophene)−Ionic Liquid Functionalized Graphene/Reduced Graphene Oxide Nanostructures: Improved Conduction and Electrochromism. *ACS Appl. Mater. Interfaces* **2011**, *3*, 1115−1126.
(26) Jiang, X.; Setodoi, S.; Fukumoto, S.; Imae, I.; Komaguchi, K.; Yano, J.; Mizota, H.; Harima, Y. An Easy One-step Electrosynthesis of Graphene/Polyaniline Composites and Electrochemical Capacitor. *Carbon* **2014**, *67*, 662−672.
(27) Tan, R.; Li, C.; Luo, J.; Kong, Y.; Zheng, W.; Yin, D. An Effective Heterogeneous L-Proline Catalyst for the Direct Asymmetric Aldol Reaction Using Graphene Oxide as Support. *J. Catal.* **2013**, *298*, 138−147.
(28) Qin, H.; Liu, J.; Chen, C.; Wang, J.; Wang, E. An Electrochemical Aptasensor for Chiral Peptide Detection Using Layer-by-Layer Assembly of Polyelectrolyte−Methylene Blue/Polyelectrolyte−Graphene Multilayer. *Anal. Chim. Acta* **2012**, *712*, 127−131.
(29) Mao, X.; Li, H. Chiral Imaging in Living Cells with Functionalized Graphene Oxide. *J. Mater. Chem. B* **2013**, *1*, 4267−4272.
(30) Wei, W.; Qu, K.; Ren, J.; Qu, X. Chiral Detection Using Reusable Fluorescent Amylose-Functionalized Graphene. *Chem. Sci.* **2011**, *2*, 2050−2056.
(31) Bu, Y.; Wang, S.; Chen, Q.; Jin, H.; Lin, J.; Wang, J. Self-Assembly of Osmium Complexes on Reduced Graphene Oxide: A Case Study Toward Electrochemical Chiral Sensing. *Electrochem. Commun.* **2012**, *16*, 80−83.
(32) Helmich, F.; Lee, C. C.; Schenning, A. P. H. J.; Meijer, E. W. J. Chiral Memory via Chiral Amplification and Selective Depolymerization of Porphyrin Aggregates. *J. Am. Chem. Soc.* **2010**, *132*, 16753−16755.
(33) Green, M. M.; Park, J.-W.; Sato, T.; Teramoto, A.; Lifson, S.; Selinger, R. L. B.; Selinger, J. V. The Macromolecular Route to Chiral Amplification. *Angew. Chem., Int. Ed.* **1999**, *38*, 3138−3154.
(34) Zhang, C.; Wang, H.; Geng, Q.; Yang, T.; Liu, L.; Sakai, R.; Satoh, T.; Kakuchi, T.; Okamoto, Y. Synthesis of Helical Poly(phenylacetylene)s with Amide Linkage Bearing L-Phenylalanine and L-Phenylglycine Ethyl Ester Pendants and Their Applications as Chiral Stationary Phases for HPLC. *Macromolecules* **2013**, *46*, 8406−8415.
(35) Pietropaolo, A.; Nakano, T. Molecular Mechanism of Polyacrylate Helix Sense Switching Across Its Free Energy Landscape. *J. Am. Chem. Soc.* **2013**, *135*, 5509−5512.
(36) Yoshida, Y.; Mawatari, Y.; Motoshige, A.; Motoshige, R.; Hiraoki, T.; Wagner, M.; Müllen, K.; Tabata, M. Accordion-Like Oscillation of Contracted and Stretched Helices of Polyacetylenes Synchronized with the Restricted Rotation of Side Chains. *J. Am. Chem. Soc.* **2013**, *135*, 4110−4116.
(37) Cui, J. X.; Zhang, J.; Wan, X. H. Unexpected Stereomutation Dependence on the Chemical Structure of Helical Vinyl Glycopolymers. *Chem. Commun.* **2012**, *48*, 4341−4343.
(38) Budhathoki-Uprety, J.; Novak, B. M. Synthesis of Alkyne-Functionalized Helical Polycarbodiimides and Their Ligation to Small Molecules Using 'Click' and Sonogashira Reactions. *Macromolecules* **2011**, *44*, 5947−5954.
(39) Zhang, X. A.; Chen, M. R.; Zhao, H.; Gao, Y.; Wei, Q.; Zhang, S.; Qin, A.; Sun, J. Z.; Tang, B. Z. A Facile Synthetic Route to Functional Poly(phenylacetylene)s with Tunable Structures and Properties. *Macromolecules* **2011**, *44*, 6724−6737.
(40) Maeda, K.; Mochizuki, H.; Osato, K.; Yashima, Y. Stimuli-Responsive Helical Poly(phenylacetylene)s Bearing Cyclodextrin Pendants That Exhibit Enantioselective Gelation in Response to Chirality of a Chiral Amine and Hierarchical Super-Structured Helix Formation. *Macromolecules* **2011**, *44*, 3217−3226.
(41) Shiotsuki, M.; Sanda, F.; Masuda, T. Polymerization of Substituted Acetylenes and Features of the Formed Polymers. *Polym. Chem.* **2011**, *2*, 1044−1058.
(42) Luo, X. F.; Deng, J. P.; Yang, W. T. Helix-Sense-Selective Polymerization of Achiral Substituted Acetylenes in Chiral Micelles. *Angew. Chem., Int. Ed.* **2011**, *50*, 4909−4912.
(43) Chen, B.; Deng, J. P.; Yang, W. T. Hollow Two-Layered Chiral Nanoparticles Consisting of Optically Active Helical Polymer/Silica: Preparation and Application for Enantioselective Crystallization. *Adv. Funct. Mater.* **2011**, *21*, 2345−2350.
(44) Luo, X. F.; Li, L.; Deng, J. P.; Guo, T. T.; Yang, W. T. Asymmetric Catalytic Emulsion Polymerization in Chiral Micelles. *Chem. Commun.* **2010**, *46*, 2745−2747.
(45) Ren, C. L.; Chen, Y.; Zhang, H. Y.; Deng, J. P. Noncovalent Chiral Functionalization of Graphene with Optically Active Helical Polymers. *Macromol. Rapid Commun.* **2013**, *34*, 1368−1374.
(46) Li, W. F.; Liu, X.; Qian, G. Y.; Deng, J. P. Immobilization of Optically Active Helical Polyacetylene-Derived Nanoparticles on Graphene Oxide by Chemical Bonds and Their Use in Enantioselective Crystallization. *Chem. Mater.* **2014**, *26*, 1948−1956.
(47) Uwada, T.; Fujii, S.; Sugiyama, T.; Usman, A.; Miura, A.; Masuhara, H.; Kanaizuka, K.; Haga, M. Glycine Crystallization in Solution by CW Laser-Induced Microbubbleon Gold Thin Film Surface. *ACS Appl. Mater. Interfaces* **2012**, *4*, 1158−1163.
(48) Schrock, R. R.; Osborn, J. A. Π-Bonded Complexes of the Tetraphenylborate Ion with Rhodium(I) and Iridium(I). *Inorg. Chem.* **1970**, *9*, 2339−2343.
(49) Deng, J. P.; Tabei, J.; Shiotsuki, M.; Sanda, F.; Masuda, T. Conformational Transition between Random Coil and Helix of Poly(*N*-propargylamides). *Macromolecules* **2004**, *37*, 1891−1896.
(50) Hummers, W. S.; Offeman, R. E. Preparation of Graphitic Oxide. *J. Am. Chem. Soc.* **1958**, *80*, 1339−1339.
(51) Yin, G.; Zheng, Z.; Wang, H.; Du, Q.; Zhang, H. Preparation of Graphene Oxide Coated Polystyrene Microspheres by Pickering Emulsion Polymerization. *J. Colloid Interface Sci.* **2013**, *394*, 192−198.
(52) Song, X.; Yang, Y.; Liu, J.; Zhao, H. PS Colloidal Particles Stabilized by Graphene Oxide. *Langmuir* **2011**, *27*, 1186−1191.
(53) Zhang, W. L.; Liu, Y. D.; Choi, H. J. Graphene Oxide Coated Core−Shell Structured Polystyrene Microspheres and Their Electrorheological Characteristics under Applied Electric Field. *J. Mater. Chem.* **2011**, *21*, 6916−6921.
(54) Meng, D.; Sun, J.; Jiang, S.; Zeng, Y.; Li, Y.; Yan, S.; Geng, J.; Huang, Y. Grafting P3HT Brushes on GO Sheets: Distinctive

Properties of the GO/P3HT Composites due to Different Grafting Approaches. *J. Mater. Chem.* **2012**, *22*, 21583−21591.
(55) Pan, Y.; Bao, H.; Sahoo, N. G.; Wu, T.; Li, L. Water-Soluble Poly(*N*-isopropyl acrylamide)−Graphene Sheets Synthesized via Click Chemistry for Drug Delivery. *Adv. Funct. Mater.* **2011**, *21*, 2754−2763.
(56) Ye, Y.-S.; Chen, Y.-N.; Wang, J.-S.; Rick, J.; Huang, Y.-J.; Chang, F.-C.; Hwang, B.-J. Versatile Grafting Approaches to Functionalizing Individually Dispersed Graphene Nanosheets Using RAFT Polymerization and Click Chemistry. *Chem. Mater.* **2012**, *24*, 2987−2997.
(57) Cano, M.; Khan, U.; Sainsbury, T.; O'Neill, A.; Wang, Z.; McGovern, I. T.; Maser, W. K.; Benito, A. M.; Coleman, J. N. Improving the Mechanical Properties of Graphene Oxide Based Materials by Covalent Attachment of Polymer Chains. *Carbon* **2013**, *52*, 363−371.
(58) Ding, P.; Su, S.; Song, N.; Tang, S.; Liu, Y.; Shi, L. Highly Thermal Conductive Composites with Polyamide-6 Covalently-Grafted Graphene by an in situ Polymerization and Thermal Reduction Process. *Carbon* **2014**, *66*, 576−584.
(59) Ma, L.; Yang, X.; Gao, L.; Lu, M.; Guo, C.; Li, Y.; Tu, Y.; Zhu, X. Synthesis and Characterization of Polymer Grafted Graphene Oxide Sheets Using a Ce(IV)/HNO_3 Redox System in an Aqueous Solution. *Carbon* **2013**, *53*, 269−276.
(60) Bai, S.; Shen, X.; Zhu, G.; Yuan, A.; Zhang, J.; Ji, Z.; Qiu, D. The Influence of Wrinkling in Reduced Graphene Oxide on Their Adsorption and Catalytic Properties. *Carbon* **2013**, *60*, 157−168.
(61) Song, C.; Liu, X.; Liu, D.; Ren, C.; Yang, W.; Deng, J. P. Optically Active Particles of Chiral Polymers. *Macromol. Rapid Commun.* **2013**, *34*, 1426−1445 and references cited therein.
(62) Li, W.; Huang, H.; Li, Y.; Deng, J. P. Particles of Polyacetylene and Its Derivatives: Preparation and Applications. *Polym. Chem.* **2014**, *5*, 1107−1118.
(63) Ferrari, A. C.; Meyer, J. C.; Scardaci, V.; Casiraghi, C.; Lazzeri, M.; Mauri, F.; Piscanec, S.; Jiang, D.; Novoselov, K. S.; Roth, S.; Geim, A. K. Raman Spectrum of Graphene and Graphene Layers. *Phys. Rev. Lett.* **2006**, *97*, 187401−187404.
(64) Guo, Y.; Guo, S.; Ren, J.; Zhai, Y.; Dong, S.; Wang, E. Cyclodextrin Functionalized Graphene Nanosheets with High Supramolecular Recognition Capability: Synthesis and Host−Guest Inclusion for Enhanced Electrochemical Performance. *ACS Nano* **2010**, *4*, 4001−4010.
(65) Mastai, Y. Enantioselective Crystallization on Nanochiral Surfaces. *Chem. Soc. Rev.* **2009**, *38*, 772−780.
(66) Medina, D. D.; Goldshtein, J.; Margel, S.; Mastai, Y. Enantioselective Crystallization on Chiral Polymeric Microspheres. *Adv. Funct. Mater.* **2007**, *17*, 944−950.